

Hierarchical space-filling in network and molecular glasses

This article has been downloaded from IOPscience. Please scroll down to see the full text article.

2007 J. Phys.: Condens. Matter 19 455213

(<http://iopscience.iop.org/0953-8984/19/45/455213>)

View [the table of contents for this issue](#), or go to the [journal homepage](#) for more

Download details:

IP Address: 129.252.86.83

The article was downloaded on 29/05/2010 at 06:31

Please note that [terms and conditions apply](#).

Hierarchical space-filling in network and molecular glasses

J C Phillips

Department of Physics and Astronomy, Rutgers University, Piscataway, NJ, 08854-8019, USA

Received 9 August 2007, in final form 10 August 2007

Published 24 October 2007

Online at stacks.iop.org/JPhysCM/19/455213

Abstract

Medium-range (nanoscale) order is the central structural factor in both the physical and technological properties of many microelectronic and microphotonic devices. Space filling and internal network stress in turn are the key factors that determine chemical trends. Instead of starting from crystals and disordering them, one can study nanoscale order starting from glasses, where chemical trends are much simpler. Special emphasis is placed on self-organized networks in the intermediate phase.

1. Introduction

Nanoscale ordering can be approached in two different ways, starting from crystals, or starting from glasses. Thanks to diffraction experiments, which provide very detailed information for crystals, it has been traditional to discuss the structure of solids starting from crystalline concepts. However, the richness and accuracy of the crystalline data base can also obscure some of the fundamental chemical trends that appear much more simply in glasses, especially network glasses. At the nanoscale limit, even for crystals the number of surface or interface atoms is comparable to the number of internal atoms that have nearest neighbors in crystalline configurations, and amorphous networks are certainly better understood starting from glasses rather than from crystals.

However appealing this glass-based program may appear, until recently it was impracticable. On the one hand, reports on glasses from glass scientists often appeared to be (and in fact, for proprietary reasons, were and are) deliberately incoherent. On the other hand, statistical mechanical models of glasses were (and still often are) based either on lattices, or on atomic models (spheres) that contained no chemical information and were useless for analyzing the fragmentary data base available in the literature [1]. While the relations between structures and properties were well understood for crystals, for all practical purposes nothing was known about network glasses beyond simple phenomenology and similarities to first-order phase transitions.

All this started to change about 1980, when a new theory appeared that analyzed network glasses as . . . networks! Not merely 'continuous random networks' [2], but as space-filling

networks subject to bond-stretching and bond-bending constraints (in the Lagrangian sense). The new theory [3, 4] begins by arranging the interatomic forces hierarchically in order of decreasing strength, and it then makes an assumption about the effects of space filling that has far-reaching consequences. The problem of space filling is then addressed inductively—by actually looking at the experimental data! (This is necessary because mathematicians believe that the problem of space filling, so far unsolved, may be insoluble by their deductive methods [5]; in fact, even the central force problem—sphere packing—is unsolved, and directional (noncentral forces) have yet to be addressed mathematically.) As we shall see through many examples, the real power of constraint theory lies in its ability to both analyze and summarize chemical trends in structure-property relations in amorphous and glassy networks, in a neoPauling style—transparent and transferable.

2. Interatomic force hierarchies and space filling

The most important structural forces in networks are rapidly varying directional covalent forces: more slowly varying ionic forces can change the packing and even alter the balance between intact and broken constraints, but in networks they otherwise have little hierarchical effect. This general statement is already a huge theoretical advance over what one can learn from Newtonian (Hamiltonian) models, whether they are restricted to parameterized central forces or actually include directional forces through first-principles total energy calculations.

Suppose that we now construct a hierarchy of covalent forces in a (for simplicity) A–B binary network glass. In addition to the obvious bond-stretching forces (easily enumerated), we will have bond-bending forces of two kinds: A–B–A and B–A–B. The number of bond-bending forces is not so easily calculated. If the coordination numbers $r(A)$ and $r(B)$ are known (for single bonds only, $r(\text{Si}) = 4$, $r(\text{Se}) = 2 \dots$, but for multiple or non-bridging bonds special rules are needed and are known in cases where enough data are available), then one might guess that the number of bond-bending forces for atom A would be $r(A)[r(A) - 1]/2$. However, this guess is wrong: the correct number is $2r(A) - 3$, which is the number of linearly independent bond angles in three dimensions. In any case, we now know how many constraints there are for each kind of force. Using radial distribution functions from diffraction data, we usually have no trouble arranging these forces hierarchically from stronger to weaker (also radially from inside to outside); the stronger forces give much narrower distributions.

Now suppose that we try to form a glass at a given composition. In an ideal gas there are $2d = N_d$ degrees of freedom/atom (position and momentum) with $d = 3$. For a glass to solidify, we must have only $N_d = d$ (vibrational motion is irrelevant). If we count the number of constraints/atom N_c and this falls in a ‘strength’ gap between the different sets of constraints, then all the stronger constraints (short-range forces) can be satisfied. Moreover, the weaker long-range (volume or van der Waals) forces can still act to compress the solid into an optimized configuration (whatever that may be). This is a *very* important point: we have constructed an algebra that will *automatically* describe the glassy configuration and many of its properties without knowing where the atoms actually are. Of course, in gases and even in liquids, such equations are a standard part of equilibrium statistical mechanics, but here we are describing a *solid* that is not even in complete equilibrium. When the gap condition is satisfied, we say that

$$N_c = N_d. \quad (1)$$

This is a global condition that has many far-reaching consequences (see Boolchand’s paper in this volume); it is a good first approximation for all network glasses, but it is modified in specific cases, depending on the geometries (chains, tetrahedra, pyramids) that are being combined to form the glass.

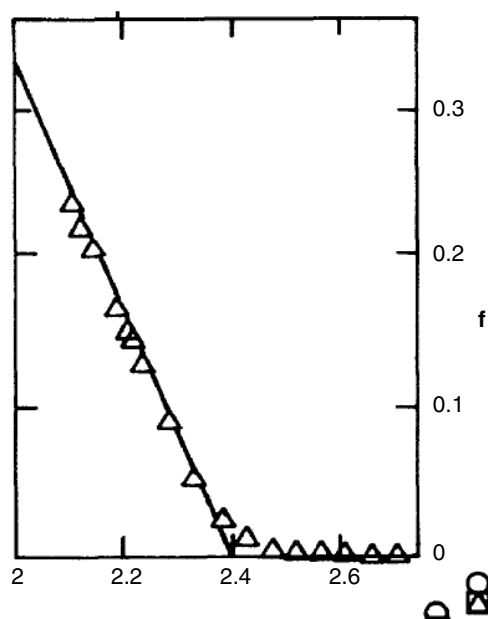


Figure 1. The fraction f of cyclical modes in a relaxed, initially tetrahedrally coordinated network, in which the average coordination number $\langle r \rangle$ has been reduced from 4 to near 2.4 by randomly deleting bonds [6].

What happens when the global condition (1) is not satisfied? If the network is relaxed and the additional or missing bonds are chosen randomly, one finds [6] a large number of zero-frequency Thorpe modes (called cyclical in classical mechanics), with the remarkably simple chemical trend shown in figure 1. Note that these modes were completely unexpected, as cyclical modes are normally associated with internal translational or rotational symmetries, and with noncentral forces there seem to be more than enough off-diagonal matrix elements in the vibrational matrix to make the lattice stable and eliminate such modes.

The 1985 discovery [6] of these cyclical modes, and their systematic variation with $\langle r \rangle$, is probably the most important theoretical advance in statistical physics since the work on the renormalization group and critical points, and it was certainly much more surprising. In reality, of course, these frequencies will become positive when weaker forces are added to the model. Nevertheless, a bulge in the vibrational density of states at low frequencies persists, which has been observed by neutron scattering, with the strength of the bulge showing the expected dependence on average coordination number $\langle r \rangle$. These hierarchically soft cyclical modes are a useful tool for analyzing the hard/soft nanocomposites that we will discuss later.

When the bonds are not randomly arranged, the network is said to be self-organized, and the single stiffness transition splits into two transitions, bounding the new Boolchand ‘phase’ of matter with nearly zero internal network stress. This new intermediate phase has no recognizable symmetries, yet it has sharp boundaries and, since its discovery, it has been found in many novel contexts (see Boolchand). Again, it is hard to overstate the importance of the intermediate phase, which even persists into supercooled liquids.

3. A few molecular applications

One of the most surprising consequences of (1) is that $\langle r \rangle$ is an excellent configuration coordinate for many glassy properties, including T_g . Starting from $r = 2$ (Se), the slope $d \log T_g / d \langle r \rangle$ measures the effectiveness of cross-linking on strengthening the network; this

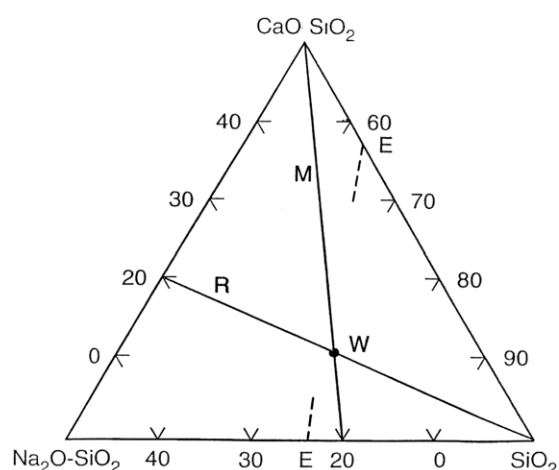


Figure 2. A ternary phase diagram for silica-soda-lime glass alloys. The line labeled M is the mean-field line for a globally stress-free network, while the line labeled R represents the local topological condition of constant ring size. The dotted line segments labeled E are eutectics. The lines M and R intersect at W, which is the composition of window glass [9].

value is a pure number $[(\ln(\langle r \rangle / 2))^{-1}]$ correctly predicted by theory for Se mixed with Si, Ge, P, As and Sb [7]. Theory also predicts that in the chalcogenide alloys the global condition (1) will usually be satisfied at the magic number $\langle r \rangle = 2.40$, which is indeed the best average value for many chalcogenide alloys (Boolchand), although local constraint corrections (special clusters with double bonding or extra constraints (edge-sharing instead of corner-sharing tetrahedra)) can shift this value by $\pm(2-3)\%$.

Although ionic effects are small in the chalcogenide glasses, one expects them to be much larger in the oxides. Their largest effect is already obvious in silica, for which $\langle r \rangle = 2.67$, yet it is an excellent glass former. This fact is often raised as a ‘killer’ criticism of constraint theory, yet it turns out to be one of its (very many) great successes. The oxygen bond-bending constraints in SiO_2 are broken, as shown by the broad distribution of oxygen bond angles, ‘an important distinction between the vitreous and crystalline forms of silica, and an important criterion for any proposed model of vitreous silica’ [8]¹. Constraint theory provides an algebraic (in fact, linear) framework for this previously isolated experimental fact, and (1) is satisfied when the oxygen bond-bending constraints are omitted from the count for $g\text{-SiO}_2$. Moreover, when the theory is generalized to include the ternary alloy system $(100-x-y)\text{SiO}_2-x\text{Na}_2\text{O}-y\text{CaO}$, one finds that the oxygen bond-bending constraints are restored. Constraint theory predicts that the ‘best’ glass (with respect to both global space-filling and smallest local interlocking ring fluctuations, which maximizes resistance to chemical attack) is obtained with $x = 16$ and $y = 10$. This is the composition of window glass [9]. This spectacular success is illustrated in figure 2.

Recently, we attempted to extend this successful analysis of the most famous (ternary) glass to the second most famous (quaternary) glass, the borosilicate pyrex [10], but the linear algebra which was accurate to 1% for window glass did not achieve 1% accuracy for pyrex ($(100-x-y-z)\text{SiO}_2, x\text{B}_2\text{O}_3, y\text{Na}_2\text{O}$ and $z\text{Al}_2\text{O}_3$). It is commonly believed, even by authors of glass handbooks, that pyrex was designed in 1915 to have small thermal expansivity (the thermal expansivity of silica is small, and $x + y + z = 20$, so that pyrex is more silica-rich

¹ The quotation is the main point (in the abstract) of this classic paper (which has more than 600 citations).

than window glass, with a three times smaller thermal expansivity). In fact, it was designed to have large resistance to mechanical shock, which our in-depth survey of the high-resolution (magic-angle spinning) ^{11}B and ^{17}O nuclear magnetic resonance (NMR) data showed demands a structure qualitatively different from that of silicates and even most other borosilicates, whereas NMR showed that window glass is nearly a ‘continuous random network’ (apart from weak correlations between Na and Ca, needed to smooth the average ring density [9]), pyrex shows a doubling of B sites which is so exceptional as to lead to a 20 year period of uncertainty, settled only by the recent 2006 repetition of the original experiment (with the same results) [10]. When we finally found these 1986–2006 data (the 1986 data were ‘hidden’ (long uncited) by uncertainty), we were most gratified, as we had already constructed a hard(silica)/soft(B, Al and Na oxides) nanocluster model that produces the desired properties. Hard/soft nanostructures are the functional basis of many (evolutionarily optimized) biostructures, for instance bone, muscle, and membrane nanosprings, and they are proving to be the structural basis for many new inorganic nanomaterials (technology imitating nature).

While biostructures lie outside the inorganic framework of this workshop, some results are worth discussing, as they demonstrate the power of analysis of optimized hierarchical space-filling networks. The key to understanding biostructure and function is (soft) hydrogen bonding between (hard) covalent backbones. Living biostructures primarily involve H, C, N and O, and it is N that produces the most complex bond bending. In this context, H bonding is hard to understand, but if one considers only simple carbohydrate molecules (alcohols, like glycerol, and saccharides, like sucrose), then one can proceed to enumerate all the constraints, and separate them into external H-bonding and internal covalent bonding. The results [11] are spectacular, as there are only a few carbohydrates that satisfy (1) (*including* external H-bonding), and these turn out to have easily recognized and remarkable properties. The beauty of the analysis is that it includes the effects of external H bonds without knowing to which external atoms the H bonds are connected. This kind of ‘precise uncertainty’ is just what is needed in the aqueous environment of life.

It should be emphasized that these results are inaccessible to conventional Newtonian Monte Carlo or molecular dynamic simulations, even for small carbohydrate molecules (10–100 atoms), because on the MDS timescale (10 ns), external hydrogen bonds ‘flicker’, and the true cooperative H-bonding structure emerges only for timescales much longer—at least milliseconds, and perhaps seconds. It is just this ‘incalculable’ long-time, low- T collective structure that constraint theory identifies. It is quite possible that the carbohydrate results will provide a platform for decoding the dynamics of large proteins containing thousands of atoms, much as other codes were broken using what cryptographers call keys—the Rosetta stone being the most famous example.

4. A few electronic applications

We come now to the real topic of this workshop—electronic nanomaterials—but why so belatedly? The answer is that there is a close relationship between electronic and molecular structures on the nanoscale, especially in optimized materials. Most workers in nanoelectronic materials already understand the electronic aspects of their subject quite well, but the atomic and molecular structures are (for the most part) mysterious. Yet it is still true, as organic chemists have long argued, that structure is function (just think of DNA!).

Probably the nature of the Si/SiO₂ interface is the most difficult and the second most important problem (after window glass) that constraint theory has solved. Of course, the issue is, why are the interfaces so ideal, and why are there so few defects—traps, or dangling bonds, at the interface? An SiO monolayer is at the Si/SiO₂ interface, and if one assumes

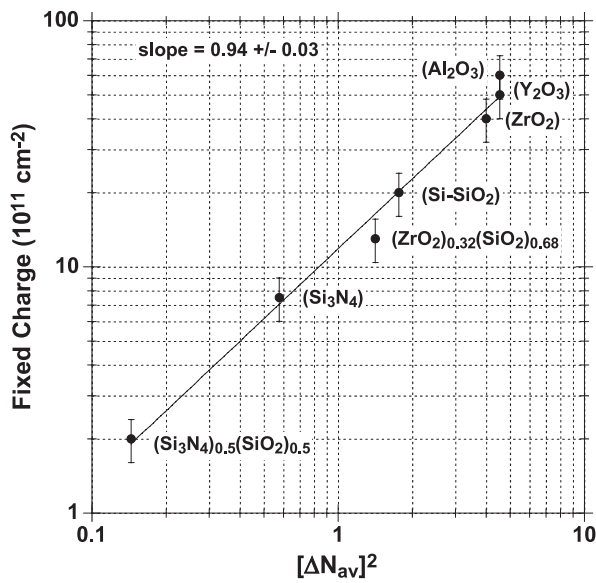


Figure 3. Fixed charge (trap density) at Si-dielectric interfaces for dielectrics of technological interest [12]. Here $\langle r \rangle = N_{av}$ is the average valence number of the dielectric and $\Delta N_{av} = N_{av} - N(\text{SiO}_2)$.

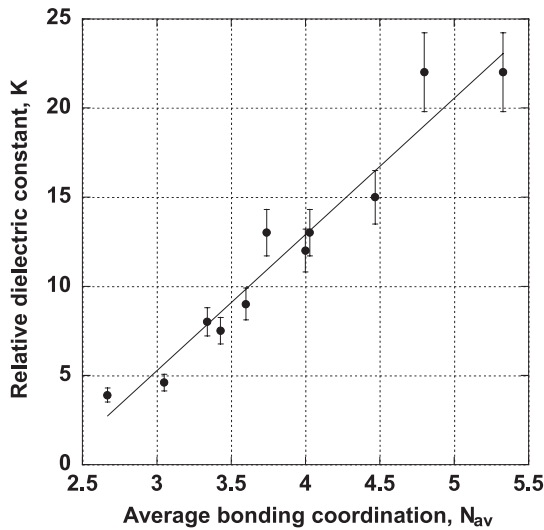


Figure 4. Dielectric constant k for many Zr- and Hf-doped dielectrics relative to silica. Here $\langle r \rangle = N_{av}$ is the average valence number of the dielectric [12].

that all the bond-bending constraints with the overconstrained Si substrate are intact, this monolayer is stressed rigid, which would presumably generate defect densities $>1\%$, as it does at all other stressed crystalline/amorphous interfaces. The problem is solved by an extension of the idea previously used for g-SiO₂. If we assume that the bending constraints involving *non-resonant* O-Si-Si interfacial bonds are broken (which is what Pauling would have done), then this monolayer is actually isostatic, that is, strain-free, which means it can be ideal. The theory [12] enables one to identify internal network stress (figure 3) as the relevant configuration coordinate for defect (charge trapping) density in SiO₂ films alloyed with other insulators. (Previous attempts used charge transfer (Pauling electro-negativity differences) as configuration coordinates, with poor results.) Another relevant interfacial parameter, the dielectric constants of Zr- or Hf-doped films, also scales with bond number (figure 4).

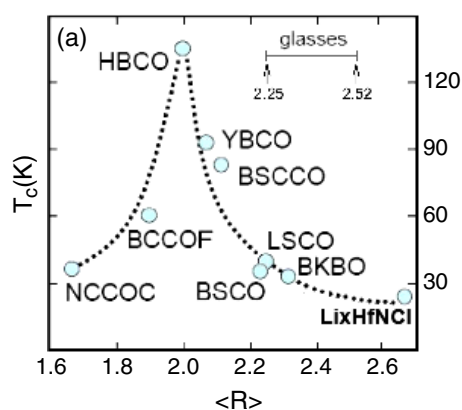


Figure 5. Perovskites ($\langle r \rangle = 2.40$) and pseudo-perovskites are only marginally stable mechanically [20], and for HTSC cuprates ($\langle r \rangle$ lies in the region of floppy networks just below the isostatic (rigid but unstressed) range determined by studies of network glasses (brackets). The peak in T_c^{\max} occurs at $\langle r \rangle = 2$, as one would expect from mean-field percolation theory. The point for BCCOF was added after the figure was originally drawn, and the original curve has not been modified. Dashed lines are guides only. Acronyms: NCCOC ($\text{Na}_x\text{Ca}_{2-x-y}\text{CuO}_2\text{Cl}_2$), BCCOF ($\text{Ba}_2\text{Ca}_3\text{Cu}_4\text{O}_8\text{F}_2$), HBCO ($\text{HgBa}_2\text{Ca}_2\text{Cu}_3\text{O}_8$), YBCO ($\text{YBa}_2\text{Cu}_3\text{O}_{6+x}$), BSCCO ($\text{Bi}_2\text{Sr}_2\text{CaCu}_2\text{O}_{8+x}$), LSCO ($\text{La}_{2-x}\text{Sr}_x\text{CuO}_4$ and $\text{La}_2\text{CuO}_{4+x}$), and BSCO ($\text{Bi}_2\text{Sr}_2\text{CuO}_{6+x}$). An extra point has been added for an Li-doped HTSC that contains no Cu. It falls on the same smooth curve, showing that it is $\langle r \rangle$ that determines the least upper bound T_c^{\max} , not the details of the chemistry: an amazing result, which shows that the (oxygen interstitial) dopant-induced superconductivity is fully adaptive (almost alive)!

(This figure is in colour only in the electronic version)

Consider next network glasses embedded in crystals: these are a new class of hard/soft electronic adaptively doped solids, previously thought to be impossible, with amazing physical properties. Impurity bands (Si:P) are examples of such networks, and they are most interesting near their metal–insulator transitions, where there is actually excellent evidence for the existence of an intermediate phase [13]. However, by far the most celebrated intermediate phases are the high-temperature superconductors (HTSCs) found in (mostly interstitial oxygen) doped cuprates, with CuO_2 planes stabilizing tetragonal pseudo-perovskite structures to prevent Jahn–Teller distortions and retain metallic character. All these materials are even more marginally stable ($\langle r \rangle \sim 2.0$) than their ferroelectric perovskite antecedents ($\langle r \rangle = 2.40$), and it turns out [14] that this practically completely determines the key parameter, which is the superconductive transition temperature T_c . This is shown for the least upper bound $T_c^{\max}(\langle r \rangle)$ in figure 5, where the abscissa is $\langle r \rangle$, now calculated literally in terms of Pauling’s resonating valence bonds (since many of the bonds are fractional, this replaces the larger and irrelevant average coordination number, just as in window glass, which used the same approach). Just how special this envelope plot is can be best appreciated by realizing that the overall scale of lattice stability is set by the melting temperature T_m , which is ~ 1000 K. Since the scatter from the smooth curve for T_c^{\max} is 10 K, the overall accuracy is $\sim 1\%$, which is quite similar to the accuracy of constraint theory for the window glass composition. Attempts to use other parameters in place of $\langle r \rangle$ (such as the average cation–anion electro-negativity difference, which measures ‘strong interactions’) result only in the scatter-shot plots that such theories have so far always produced.

My final adaptive example again concerns reversibility windows. Ordinarily, glass technology likes compositions near the center of the reversibility window, as these are the

most stable. $\text{Ge}_2\text{Sb}_2\text{Te}_5$ (GST) is especially interesting, as it is the material of choice in digital versatile disc-random access memories (DVD-RAM). It has been argued [15] that GST consists of well-defined rigid building blocks that are randomly oriented in space, consistent with cubic symmetry. Laser-induced amorphization results in a drastic shortening of covalent bonds and a decrease in the mean-square relative displacement, demonstrating a substantial increase in the degree of short-range ordering, in sharp contrast to the amorphization of typical covalently bonded solids. This transition, which can also be induced by a hydrostatic pressure of 5–6 GPa, is ascribed to an umbrella-flip of Ge atoms from an octahedral position into a tetrahedral position without the rupture of strong covalent bonds.

This description of GST leaves an important question unanswered: with such a large structural change, why are the bonds not ruptured at the interface between the transformed amorphous and unexposed crystalline regions? Two answers have been suggested: (I) total energy calculations of different GeSb_2Te_4 (not GST) crystal structures show similar energies for crystals with tetrahedral and octahedral local Ge environments [16], and (II) a careful count of all the bonding constraints in an amorphous GST film studied by extended x-ray absorption fine structure (EXAFS) spectroscopy shows that the ideal glass-forming condition (1) is satisfied within 2% [17] (the error could be caused by uncertainties in the EXAFS deconvolution). While it is true that the precision of total energy calculations is now excellent, such models (I) are always questionable, as one cannot be sure that any combination of the specific atomic crystalline configurations is representative of the amorphous structure. (Here, for example, (I) GeSb_2Te_4 (not GST) is overconstrained by 20%, which is an error ten times larger than the (II) EXAFS experimental uncertainties.) Constraint counting, on the other hand, is backed up by all the experience with the reversibility window in both chalcogenide and oxide bulk glasses, 1% accuracy in the ternary composition of window glass, the Si/SiO₂ interface, etc: in other words, it is not only simple and transparent, but it is also a very general and extremely effective phenomenology (often accurate to 1%), well tested not only for bulk glasses, but also for the interfaces between amorphous and crystalline networks.

References

- [1] Mysen B and Richet P 2005 *Silicate Glasses and Melts* (Amsterdam: Elsevier)
- [2] Zachariasen W H 1932 *J. Am. Chem. Soc.* **54** 3841
- [3] Phillips J C 1979 *J. Non-Cryst. Sol.* **34** 153
- [4] Boolchand P, Lucovsky G, Phillips J C and Thorpe M F 2005 *Phil. Mag.* **85** 3823
- [5] Singh S 1998 *Fermat's Enigma* (New York: Anchor Books)
- [6] He H and Thorpe M F 1985 *Phys. Rev. Lett.* **54** 2107
- [7] Kerner R and Micoulaut M 1997 *J. Mol. Liquids* **71** 175
- [8] Mozzzi R L and Warren B E 1969 *J. Appl. Cryst.* **2** 164
- [9] Kerner R and Phillips J C 2001 *Solid State Commun.* **117** 47
- [10] Phillips J C and Kerner R, unpublished
Prasad S, Clark T M, Sefzik T H, Kwak H T, Gan Z H and Grandinetti P J 2006 **352** 2834
- [11] Phillips J C 2006 *Phys. Rev. B* **73** 024210
- [12] Lucovsky G and Phillips J C 2004 *Appl. Phys. A* **78** 453
- [13] Phillips J C 1999 *Solid State Commun.* **109** 301
- [14] Phillips J C 2007 *Phys. Rev. B* **75** 214503
- [15] Kolobov A V, Fons P, Frenkel A I, Ankudinov A L, Tominaga J and Uriga T 2004 *Nat. Mater.* **3** 703
Kolobov AV *et al* 2006 *Phys. Rev. Lett.* **97** 035701
Hosokawa S *et al* 2007 *Appl. Phys. Lett.* **90** 131913
- [16] Welnic W, Pamungkas A, Detemple R, Steimer C, Blugel S and Wuttig M 2006 *Nat. Mater.* **5** 56
- [17] Baker D A, Paesler M A, Lucovsky G, Agarawal S C and Taylor P C 2006 *Phys. Rev. Lett.* **96** 255501